Journal of Materials Chemistry A

PAPER

View Article Online
View Journal | View Issue

Cite this: J. Mater. Chem. A, 2015, 3, 19061

A gamma fluorinated ether as an additive for enhanced oxygen activity in Li–O_2 batteries†

Olivia Wijaya,[a] Pascal Hartmann,[b] Reza Younesi,[c] Iulius I. E. Markovits,[d] Ali Rinaldi,[a] Jürgen Janek[b] and Rachid Yazami*[d]

Received 11th May 2015
Accepted 7th August 2015

DOI: 10.1039/c5ta03439f

www.rsc.org/MaterialsA

Perfluorocarbons (PFCs) are known for their high O_2 solubility and have been investigated as additives in Li–O_2 cells to enhance the cathode performance. However, the immiscibility of PFCs with organic solvents remains the main issue to be addressed as it hinders PFC practical application in Li–O_2 cells. Furthermore, the effect of PFC additives on the O_2 mass transport properties in the catholyte and their stability has not been thoroughly investigated. In this study, we investigated the properties of 1,1,1,2,2,3,3,4,4-nonafluoro-6-propoxyhexane (TE4), a gamma fluorinated ether, and found it to be miscible with tetraglyme (TEGDME), a solvent commonly used in Li–O_2 cells. The results show that with the TE4 additive up to 4 times higher O_2 solubility and up to 2 times higher O_2 diffusibility can be achieved. With 20 vol% TE4 addition, the discharge capacity increased about 10 times at a high discharge rate of 400 mA g_C^{-1}, corresponding to about 0.4 mA cm^{-2}. The chemical stability of TE4 after Li–O_2 cell discharge is investigated using ^{1}H and ^{19}F NMR, and the TE4 signal is retained after discharge. FTIR and XPS measurements indicate the presence of Li_2O_2 as a discharged product, together with side products from the parasitic reactions of LiTFSI salt and TEGDME.

Introduction

A high O_2 solubility in the catholyte is a desirable property in Li–O_2 batteries since the cathode reaction consists of O_2 reduction to form Li_2O_2.[1–5] In fact, Read *et al.* found that the discharge capacity of Li–O_2 cells increased with the O_2 partial pressure and with the Bunsen coefficient (cm^3 O_2 per cm^3 solution) of the catholyte.[6,7] Optimized partial filling of cathode pores with a liquid electrolyte also will improve the discharge kinetics.[8]

PFCs are used in various biological applications, including in artificial blood due to their high O_2 solubility.[9–11] Therefore, PFCs are attractive candidates as additives to increase the O_2 activity in the catholyte of a Li–O_2 battery. In fact, perfluoroheptane dissolves about 5.6 times more O_2 than tetraglyme (TEGDME), a common solvent in Li–O_2 batteries. TEGDME shows good stability with Li metal and a wide electrochemical stability window.[12–14] The O_2 solubility in perfluoroheptane was measured by Tominaga *et al.*[15] from the O_2 solubility given as a mole fraction (x_{O_2}), and they reported $x_{O_2} = 55.5 \times 10^{-4}$, which corresponds to a Bunsen coefficient of $\alpha = 0.553$. Read *et al.*[16] found a lower Bunsen coefficient of $\alpha = 0.0993$ in TEGDME.

The beneficial effect of PFC additives on metal–O_2 battery cell performance enhancement has been reported in the literature. In pioneering work submitted to a US patent, Yazami showed an increase of the open-circuit voltage in cells with PFC additives in aqueous electrolytes.[17] This increase necessarily means that the fluorocarbon additive influences the cell reaction. Later, Balaish *et al.*[1,18] and Zhang *et al.*[2] reported an increase in the discharge capacity of Li–O_2 battery cells with PFC and partially fluorinated compound additives, respectively. Further, Wang *et al.* found an increase in the current density during O_2 reduction by dispersing perfluorotributylamine in propylene carbonate solvent.[4] A recent study by Nishikami *et al.*[5] showed around 1.5 times capacity increase when dissolving 60 wt% perfluorohexyl bromide with lithium perfluorooctane sulfonate in tetraglyme. We also reported an enhanced current and discharge capacity with 1-methoxyheptafluoropropane additive in DME and TEGDME based battery electrolytes with a rotating ring disk electrode (RRDE) and a Li–O_2 cell.[3]

The limited miscibility of PFCs in organic solvents is one of the main issues in Li–O_2 cell application. One proposed strategy to overcome this issue is a dispersion of the liquid medium.[4] However, this approach does not meet the long term stability requirement of the two-phase liquid/liquid dispersion. The other strategy we have pursued is to use PFCs with a lower degree of fluorination as they may provide a good tradeoff between solubility in ethers and O_2 dissolution capability.[3]

[a]TUM CREATE, 1 CREATE Way, #10-02, Singapore 138602
[b]Institute of Physical Chemistry, Justus-Liebig-Universität Gießen, Heinrich-Buff-Ring 58, 35392 Gießen, Germany
[c]Department of Chemistry-Ångström Laboratory, Uppsala University, Box 538, SE-751 21 Uppsala, Sweden
[d]Energy Research Institute at Nanyang Technological University, 1 CleanTech Loop, #06-04 CleanTech One, Singapore 637141. E-mail: rachid@pmail.ntu.edu.sg

† Electronic supplementary information (ESI) available. See DOI: 10.1039/c5ta03439f

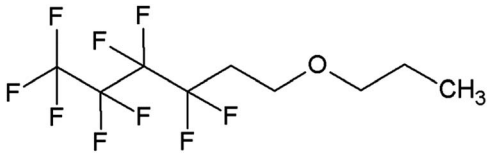

Fig. 1 Molecular structure of 1,1,1,2,2,3,3,4,4-nonafluoro-6-propoxyhexane (TE4).

Another important requirement for PFC additives is good chemical stability in the Li–O_2 cell environment. In fact, superoxide radicals are reported to form in the course of O_2 reduction and should account for the instability of solvents commonly used in Li–O_2 batteries, including carbonates and glymes.[19–26] Recently, we reported on the plausible instability of 1-methoxyheptafluoropropane by using a RRDE and cyclic voltammetry.[3]

In this work, we investigated a gamma-fluorinated ether, 1,1,1,2,2,3,3,4,4-nonafluoro-6-propoxyhexane (TE4) (Fig. 1), as an additive in Li–O_2 batteries. This compound is expected to have greater stability toward the superoxide radicals compared to 1-methoxyheptafluoropropane (an alpha-fluorinated ether) as predicted by the DFT calculation.[27] The O_2 solubility of this compound is also expected to be high (47.76 cm^3/100 ml) by the calculation developed by Lawson *et al.*[28] Furthermore, TE4 is miscible with TEGDME and lithium up to a considerable amount (~20 vol%). Therefore, the issue of dispersion instability and appropriate surfactant could be avoided. The O_2 uptake in pure TE4 and TE4 solutions in tetraglyme of various concentrations is measured here. We show the beneficial effects of the TE4 additive on the discharge capacity and on the rate capability in Li–O_2 cells. The stability of the TE4 upon discharge is investigated using NMR spectroscopy. The discharged products are investigated using XPS and FTIR spectroscopy.

Experimental section

Electrolyte preparation

TEGDME was purchased from Sigma-Aldrich and distilled prior to use to remove impurities. The solvent is further dried over 3 Å molecular sieves. 99.5% LiTFSI from Solvay was dried at 60 °C under 10–3 mbar vacuum for 3 days. 1,1,1,2,2,3,3,4,4-Nonafluoro-6-propoxyhexane (HFE-TE4-O-C3), >99%, (TA4) was obtained from Fluoryx Inc. Its structure is presented in Fig. 1. TE4 is dried over 3 Å molecular sieves in an argon filled glovebox. The electrolyte mixture is prepared inside the argon glovebox with <1 ppm H_2O and O_2. The electrolyte water content is analyzed by the Karl Fischer titration technique and it is found to be below 20 ppm. The ionic conductivity was measured using a conductivity meter CyberScan Series 600 from Eutech Instruments and found to be 0.6 mS cm^{-1} for 0.1 M LiTFSI:TEGDME. The ionic conductivity of the electrolytes with the TE4 additive does not differ significantly. The viscosity of TEGDME is 4.05 cP.[29]

Cathode fabrication and cell assembly

The cathodes were prepared by coating a slurry of graphitized carbon black (Sigma-Aldrich) (80 wt%) with a PTFE binder (Sigma-Aldrich) (20 wt%) onto a Celgard 2320 separator. The slurry was prepared by sonicating (Hielscher, UP200S) the carbon and binder in isopropanol for 5 minutes followed by stirring for 30 minutes using a Heidolph Silent Crusher homogenizer at a high speed of 10 000 rpm. A 14 mm cathode disk was cut and dried at 90 °C for 12 hours before being transferred to the glovebox. Stainless steel mesh was utilized as the current collector. The cathodes are 1.5–1.6 mg in weight, ~10 μm in thickness and with a carbon loading of 0.97–1.03 mg cm^{-2}. Cells were assembled in an Ar filled glovebox (O_2 < 1 ppm, H_2O < 1 ppm). An additional Celgard separator is placed between the carbon cathode and the lithium metal anode. The discharge experiments were conducted in ECC-Air laboratory cells produced by EL-Cell GmbH[30] with a Kel-F O-ring to avoid water permeation into the cell.[31] O_2 was introduced into the cell with a stainless steel tubing for one hour at 0.5 ml min^{-1} prior to discharge; the cells were discharged using an Arbin Battery Tester.

Physical characterization

^1H and ^{19}F NMR spectra of the catholyte were recorded before and after discharge to investigate the stability of the additive. The ^1H NMR spectra were measured in $CDCl_3$ on an Avance I 400 MHz NMR spectrometer. For the ^{19}F NMR spectra, the sample was prepared in DMSO-d6 and measured on an Avance 300 MHz NMR spectrometer. XPS measurements were performed on a PHI 5500 spectrometer (Perkin Elmer Physical Electronics) using monochromatized Al-Kα radiation (1487 eV) and an electron emission angle of 45°. The probing area was approximately 2 × 4 mm^2. All spectra were energy calibrated by using the C–C peak of carbon black at a binding energy of 284.5 eV. The samples were washed with DME to remove the remaining electrolyte solvent and salt. FTIR measurements were performed using a frontier from Perkin Elmer in the reflectance mode using EasiDiff™ accessories. The spectra were transformed using the Kubelka–Munk equation to compensate the differences with the standard spectra. The discharged cathode was washed with DME and mixed with vacuum dried KBr inside the glovebox to avoid any reaction during sample preparation.

O_2 uptake measurements

The O_2 uptake measurements were performed using a cross fitting setup equipped with a PAA-33X absolute pressure sensor (Omega), an O_2 reservoir, and a vacuum pump. 5 ml of the electrolyte mixture was placed in a glass flask and degassed by exposing it to vacuum. The details of the setup and experimental procedure can be found in ref. 32. The determination of the Henry constant was done by increasing the O_2 partial pressure repeatedly and measuring the pressure drop due to O_2 uptake. The diffusion coefficient was measured by using convection free O_2 absorption in thin liquid films, and the data were analyzed by using a 1D diffusion model reported by Hou *et al.*[33] The pressure decay profile was recorded until a steady state plateau was obtained.

Result and discussion

O_2 concentration and diffusion coefficient measurements

Fig. 2 shows the molar concentration of O_2 in the TEGDME solvent with varying TE4 additive contents as a function of pressure at room temperature. The Henry constant (H_{O_2}) is determined by the linear fit of this plot as in eqn (1). The diffusion of O_2 (D_{O_2}) is measured for the TEGDME solvent, TEGDME with 20 vol% TE4, and pure TE4 additive. The O_2 diffusion profile and the equation model for the fitting can be found in S1.† The results for O_2 concentration and diffusion are summarized in Table 1.

$$C_{O_2} = H_{O_2} \times P_{O_2} \quad (1)$$

C_{O_2}: O_2 concentration, H_{O_2}: Henry's constant, P_{O_2}: O_2 pressure

The data clearly show that the pure TE4 additive has about a four times higher Henry constant H_{O_2} compared to pure TEGDME. Addition of 10 vol%, 20 vol%, and 60 vol% TE4 increases H_{O_2} by factors of 1.2, 1.5, and 3, respectively, compared to TEGDME alone. H_{O_2} increases linearly with the TE4 concentration (Fig. S2†). Moreover, the D_{O_2} in the pure TE4 additive is about 2 times higher than that in the TEGDME solvent. However, surprisingly, the D_{O_2} in the 20 vol% TE4 additive remains unchanged compared to pure TEGDME. The addition of LiTFSI, especially at a low concentration of 0.1 M, will not change H_{O_2} significantly, as evidenced from our previous results.[32,34]

We calculated the O_2 solubility based on the fluorocarbon chemical structure by using the method developed by Lawson *et al.*[28] and compared it with our experimental result. The O_2 solubility (cm^3/100 ml of liquid) at 25 °C was found to be of 47.76, which is close to our result of 45.45 ± 0.15. The details of the calculation can be found in S3.†

The main motivation for incorporating fluorinated additives into the metal–O_2 battery is the enhancement of O_2 concentration and mass transport. However, most of the previous studies either did not quantify the increase in O_2 concentration and diffusion coefficient nor did they quantify them beyond using

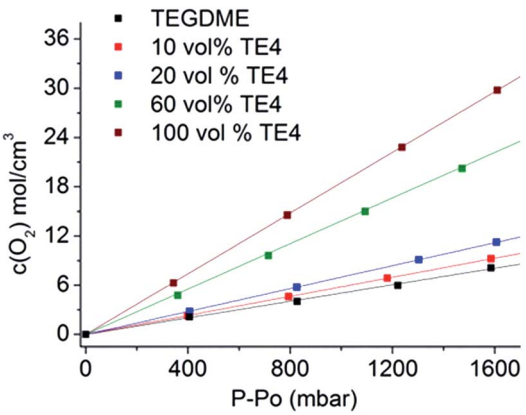

Fig. 2 O_2 concentration for various TE4 additive concentrations in the TEGDME solvent as a function of O_2 pressure. The Henry constant is determined by the linear fit.

Table 1 Henry constant and diffusion coefficient of O_2 for TEGDME with different additive concentrations determined from oxygen take-up experiments

Solvents	[TE4] (M)	Density (g cm^{-3})	H_{O_2} (mol m^{-3} bar^{-1})	$D_{O_2}/10^{-5}$ (cm^2 s^{-1})
TEGDME	0	1.003	4.8 ± 0.2	2.60 ± 0.03
TEGDME + 10 vol% TE4	0.43	1.032	5.8 ± 0.2	—
TEGDME + 20 vol% TE4	0.86	1.180	7.0 ± 0.2	2.62 ± 0.06
TEGDME + 60 vol% TE4	2.57	1.263	14.2 ± 0.4	—
TE4	—	1.313	18.6 ± 0.6	5.10 ± 0.06

electrochemical techniques such as Rotating Ring Disk Electrodes (RRDEs).[3,4] The rotating ring disk electrode has several limitations such as salt precipitation at high fluorocarbon concentration, high volume of sample, and also problematic data interpretation due to the probability of electrolyte/additive instability in the O_2 environment. Therefore, we used pressure dynamic measurements to quantify O_2 concentration and the diffusion of the fluorocarbon additive. This approach requires a relatively low amount of sample and provides clear data interpretation since only O_2 gas is utilized for the measurements.[32]

Discharge at various rates

The maximum amount of miscible TE4 in 0.1 M LiTFSI:-TEGDME is 20 vol% (0.86 M). Above 20 vol% TE4 concentration, LiTFSI will precipitate. Electrolyte mixtures with different TE4 additive concentrations (0–20 vol%) were therefore tested during discharge at various rates.

Fig. 3a shows that at 100 mA g_C^{-1} (about 0.1 mA cm^{-2}), the Li–O_2 cell with 0.1 M LiTFSI:TEGDME electrolyte yields 375 mA h g_C^{-1} capacity with a voltage plateau of ~2.55 V. The capacity increases by ~25 mA h g_C^{-1} and ~50 mA h g_C^{-1} by adding 10 vol% and 20 vol% TE4, respectively. However, there is no unequivocal change in discharge voltage observed.

Fig. 3b shows the discharge profile at 200 mA g_C^{-1} (about 0.2 mA cm^{-2}) current rate. The discharge capacity of the cell with 0.1 M LiTFSI:TEGDME electrolyte decreases to 300 mA h g_C^{-1} and the discharge voltage decreases to 2.42 V. However, the discharge voltage increased to ~70 mV with the 20 vol% TE4 additive as compared to the TE4 free electrolyte. Fig. 3c displays the discharge profile at a high current rate of 400 mA g_C^{-1} (about 0.4 mA cm^{-2}). The TE4 free cell yielded a low capacity of 25 mA h g_C^{-1}. The latter increased to 90 mA h g_C^{-1} and 225 mA h g_C^{-1} in electrolytes with 10 vol% and 20 vol% TE4, which is about 3.5 times and about 10 times higher, respectively.

The effect of the TE4 additive is more paramount at a high discharge rate, where the O_2 supply is critical. Our improved discharge performance data are in agreement with those of Read *et al.* owing to the enhanced O_2 solubility.[2] Read *et al.* used PC as a solvent[2] which is unstable under O_2 reduction and did not address the stability issue of the PFC additive.[35] In this work, the TEGDME is used due to its higher stability toward

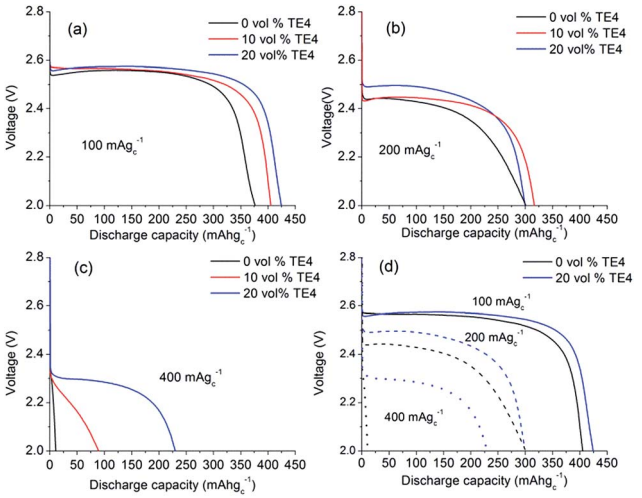

Fig. 3 Galvanostatic discharge profiles of Li–O_2 cells at current densities of (a) 100 mA g_C^{-1} (about 0.1 mA cm^{-2}), (b) 200 mA g_C^{-1} (about 0.2 mA cm^{-2}), and (c) 400 mA g_C^{-1} (about 0.4 mA cm^{-2}) with 0.1 M LiTFSI in TEGDME containing 0, 10, and 20 vol% TE4 additive. (d) A summary of the effect of the TE4 additive by comparing the electrolyte with 0 and 20 vol% TE4 at various discharge rates.

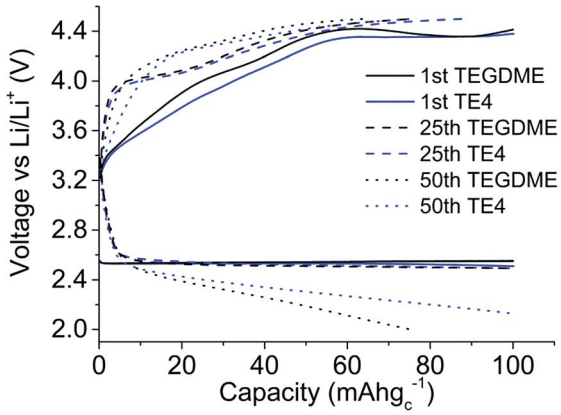

Fig. 4 1st (solid line), 25th (dashed line) and 50th (dotted line) charge and discharge cycle profiles for the Li–O_2 cell using 0.1 M LiTFSI: TEGDME (black) and 0.1 M LiTFSI:TEGDME + 20 vol% TE4 additives (blue). The cells were galvanostatically discharged at 100 mA g_C^{-1} up to 100 mA h g_C^{-1} or 2 V and charged at 100 mA g_C^{-1} up to 100 mA h g_C^{-1} or 4.5 V, whichever limit reached earlier.

superoxides compared to PC.[36] As discussed in the next section, TE4 is relatively stable towards oxidation, which results in good performance during the first discharge in the Li–O_2 battery. Fig. 4 shows the cycle performance of the Li–O_2 cell with 0.1 M LiTFSI:TEGDME with and without the addition of the TE4 additive. We found out that the cell with the TE4 additive has a longer cycle life than that with the TEGDME only additive. At the 50th cycle, the cell with the TE4 additive can still be discharged up to 100 mA h g_C^{-1} while the cell without the additive can only be discharged up to 76 mA h g_C^{-1}. The charge voltage is also consistently slightly lower for the cell with the TE4 additive. Nevertheless, the exact mechanism of discharge and charge for the cell with and without the TE4 additive is beyond the scope of this work.

Stability of the TE4 additive

The chemical stability of the fluorocarbon additive in Li–O_2 cells has not been investigated although it is a pre-requisite for battery application.

In this section, we will first evaluate the electrochemical window of the electrolyte with the TE4 additive in an argon environment. Subsequently, the stability of the TE4 additive is evaluated using ^{1}H NMR and ^{19}F NMR for the electrolyte before and after discharge.

Fig. 5 shows the cyclic voltammogram (CV) in argon for the cell with and without the TE4 additive in the electrolyte at 1 mV s^{-1} from 2.8 V to a lower potential of 2 V or 1.5 V and then to 4.5 V. The CV profiles of cells with the TE4 additive coincide with the CV profile of the cell with only 0.1 M LiTFSI:TEGDME within 2–4.5 V and 1.5–4.5 V. There is no additional reduction or oxidation peak observed. This signifies that the TE4 additive is electrochemically stable within the above mentioned voltage range. This is especially important since we tested the Li–O_2 cell within 2–4.5 V. The ^{1}H and ^{19}F NMR spectra recorded on pure TE4 are in agreement with the literature (the description of the spectra can be found in S6†). As shown in Fig. 6, the ^{1}H NMR spectra after discharge is quasi-identical to the pure TE4 one, denoting a high stability. This is further evidenced by ^{19}F-NMR data displayed in Fig. 7.

All signals can be assigned to TE4 with the exception of the one at $\delta = -78.93$ ppm corresponding to LiTFSI.[37] However, the integral peak ratio of CF_3 (−80.94 ppm) : LiTFSI (−78.93 ppm) increased after discharge from 1 : 0.2 to 1 : 0.3. Therefore, TE4 shows considerably higher stability during O_2 reduction when compared to the 1-methoxyheptafluropropane additive we reported on.[3] In fact, the ^{1}H and ^{19}F signals from 1-methoxyheptafluoropropane completely disappeared after discharge (S4 and S5†) as a sign of instability.

The increased stability is attributed to the synergistic effect of the two alkyl chains besides the ether group in TE4.

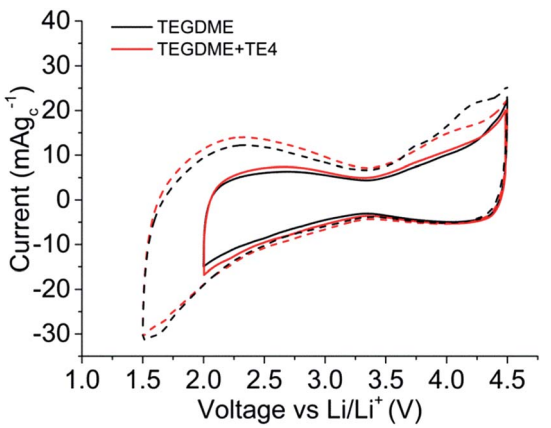

Fig. 5 Electrochemical stability window of 0.1 M LiTFSI:TEGDME (black) and 0.1 M LiTFSI:TEGDME + 20 vol% TE4 (red) within potential windows of 2 V to 4.5 V (solid line) and 1.5 V to 4.5 V (dashed line) *vs.* Li/Li$^+$.

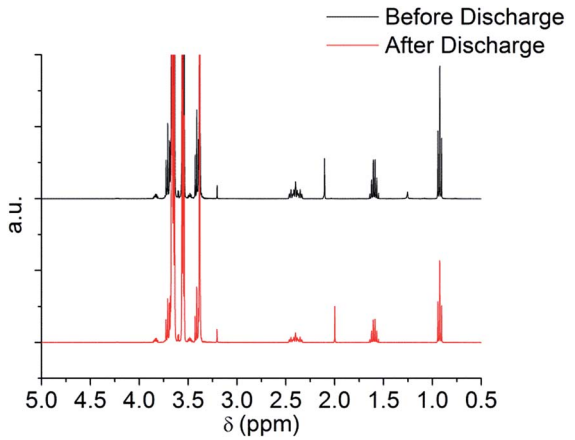

Fig. 6 ^{1}H NMR before and after discharge at 100 mA g_C^{-1} to 2 V of 0.1 M LiTFSI:TEGDME + 20 vol% TE4.

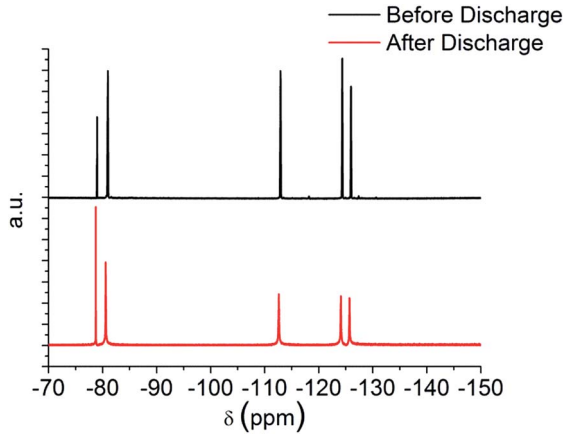

Fig. 7 ^{19}F NMR before and after discharge at 100 mA g_C^{-1} to 2 V of 0.1 M LiTFSI:TEGDME + 20 vol% TE4.

Theoretical calculations have shown that with fluorination a decreased susceptibility of the CF_2–O towards an attack by O_2^- is expected. However, the fluorination leads to a decreased reaction barrier for an attack to the neighboring bond, *i.e.* CH_3–O for 1-methoxyheptafluoropropane and therefore an increased instability in the presence of superoxides.[20] The ethylene bridge in TE4 prevents this destabilization by balancing the electron deficiency created by the fluorinated alkyl group and helps prevent an attack by the superoxide anion radical on the CH_2–O group. Additionally, this effect is supported by the *n*-propoxy group of the TE4 additive compared to the smaller methyl group.[27]

Discharge product characterization

FTIR and XPS were used to reveal the nature of the discharged product formed. Fig. 8 shows the IR spectra of the discharged cathode. The signal at 400–700 cm^{-1} indicates the presence of Li_2O_2, together with side products such as Li_2CO_3 at 1392–1570 cm^{-1}. There is no strong indication that LiOH is present as the discharge product. The presence of a C–F signal at 1263–1141 cm^{-1} indicates that the PTFE binder utilized is stable during discharge in Li–O_2. Upon exposure to air for 15 minutes (Fig. S7†), the IR signal in the 1392–1570 cm^{-1} region and 869 cm^{-1} increases, indicating the presence of a discharged product that is unstable in air, likely to be Li_2O_2. To further confirm the chemistry of the discharged product, XPS analysis was done on the discharged cathode with and without the TE4 additive. Fig. 9 shows the XPS core level spectra of the pristine cathode and discharged cathodes with and without the TE4 additive. The O1s spectra of both discharged samples indicate the formation of Li_2O_2 at a binding energy of 531.5 eV, as well as, side products such as $-CO_3$, C=O, C–O, and O–F containing compounds at binding energies of 532.1, 533.5, and 534.3 eV, respectively.[38,39] C1s, F1s, and Li1s spectra confirm the formation of such compounds, and in addition, F1s spectra show the formation of LiF on the discharged cathodes.

The presence of a peak with a very high binding energy at above 534 eV in the O1s spectra suggests that O is bonded to highly electronegative elements such as F. This consequently resulted in the appearance of a peak with a very high binding energy, above 692 eV, in the F1s spectra. F–O containing compounds could, for example, be formed due to the decomposition of $LiPF_6$ resulting in the appearance of a peak at above 534 eV, as reported in different literature studies.[40,41] The presence of O–F in compounds at a high binding energy of ~692 eV in the F1s spectra and at above 534 eV in the O1s spectra has also been reported in the literature, for example, the formation of the Si–O–F bond during the SiO_2 etching process.[42–44]

In order to understand the origin of the O–F signals formed, we deconvoluted and quantified the F1s spectra. The result is shown in Table 2.

We found that the quantity of the O–F bond formed in the cathode discharged in the TEGDME electrolyte is similar to the one discharged in the TEGDME + TE4 additive. This indicates that the O–F bond mostly originates from other F-containing compounds such as the LiTFSI salt, in agreement with the literature, showing that LiTFSI decomposed during discharge in Li–O_2 batteries.[45–49] LiTFSI, similar to the $LiPF_6$, which decomposes to $Li_xPF_yO_z$, may decompose to O and F containing

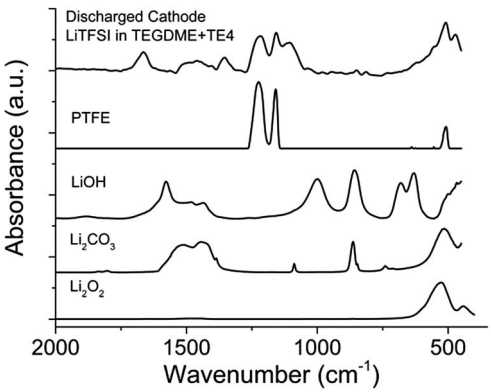

Fig. 8 FTIR spectra of the cathode discharged using 0.1 M LiTFSI: TEGDME + 20 vol% TE4 electrolyte at 100 mA g_C^{-1}. Comparison of LiOH, Li_2CO_3, Li_2O_2 and PTFE FTIR spectra is provided.

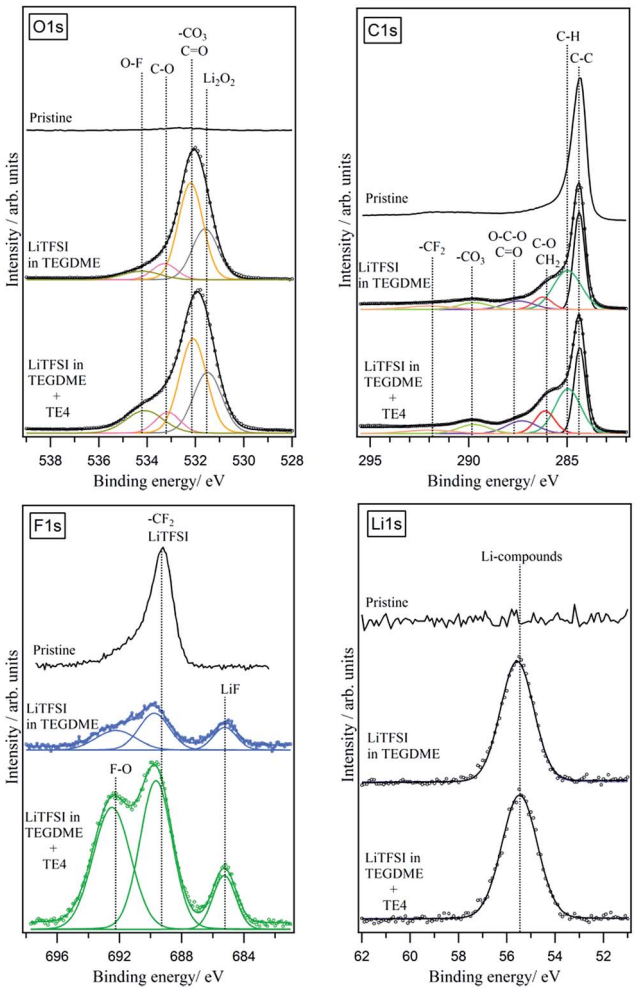

Fig. 9 XPS O1s, C1s, F1s, and Li1s spectra of pristine and discharged cathodes with and without the TE4 additive. The cathode was discharged at 100 mA g_C^{-1}.

compounds.[40,41,50] The XPS results show that the TE4 addition does not result in additional discharge products from the parasitic reaction.

In summary, the spectroscopy data agrees with those of the TE4 additive, a γ-fluorinated ether, which has a good stability in Li–O_2 batteries, considerably enhanced compared to an α-fluorinated ether. The ^{1}H and ^{19}F NMR results show that the additive is retained after discharge in the Li–O_2 battery and no additional product dissolved in the electrolyte is observed. FTIR and XPS data confirmed the formation of Li_2O_2 during discharge. Side products such as –CO_3, C=O, C–O, and O–F containing compounds and LiF are also detected, most likely from the LiTFSI salt and TEGDME decomposition. The decomposition of LiTFSI is supported by the change of the LiTFSI peak ratio in the ^{19}F NMR result after discharge.

Table 2 Peak quantification for the deconvoluted F1s spectra

Electrolyte	LiF	CF_2 (PTFE) and LiTFSI	F–O
0.1 M LiTFSI:TEGDME	25%	32%	43%
0.1 M LiTFSI:TEGDME + TE4	25%	35%	40%

Conclusions

We showed the effect of the TE4 additive in enhancing the discharge performance of Li–O_2 batteries, which confirms the potential of utilizing dissolved fluorocarbon additives in this chemistry. The addition of 20 vol% TE4 resulted in a discharge capacity of 400 mA h g_C^{-1} enhanced by a factor of 10. To the best of our knowledge, this is the first time also that the O_2 solubility and diffusion of the TE4 compound are reported.

The electrochemical performance improvement is related to enhanced O_2 solubility and mass transport in the TEGDME solvent as evidenced by a pressure change measurement technique.

NMR analysis of the electrolyte before and after discharge showed the considerably enhanced TE4 chemical stability against superoxide radical attack during discharge, compared to the previous additive we reported. We also showed that Li_2O_2 is present after discharge and no additional product is detected from the parasitic reactions with the TE4 additive. These encouraging results are the first step in finding optimized additives especially for higher discharge rates, where not only the stability of such additives is required but also the fast O_2 mass transport.

Acknowledgements

This research project is funded by the National Research Foundation Singapore under its Campus for Research Excellence and Technological Enterprise (CREATE) programme. We thank Solvay company for providing LiTFSI salt. P. H. thanks *Fonds der Chemischen Industrie* (FCI) for a Ph.D. scholarship. J. J. acknowledges support by the Laboratory of Materials Research (LaMa and ElCh).

Notes and references

1 M. Balaish, A. Kraytsberg and Y. Ein-Eli, *ChemElectroChem*, 2014, **1**, 90.
2 S. S. Zhang and J. Read, *J. Power Sources*, 2011, **196**, 2867.
3 A. Rinaldi, Y. Wang, K. S. Tan, O. Wijaya and R. Yazami, in *Advances in Batteries for Medium and Large-Scale Energy Storage*, ed. C. Menictas, M. Skyllas-Kazacos and T. M. Lim, Woodhead Publishing, Cambridge, 1st edn, 2014, pp. 419–430.
4 Y. Wang, D. Zheng, X. Yang and D. Qu, *Energy Environ. Sci.*, 2011, **4**, 3697.
5 Y. Nishikami, T. Konishi, R. Omoda, Y. Aihara, K. Oyaizu and H. Nishide, *J. Mater. Chem. A*, 2015, **3**, 10845.
6 S. S. Zhang, K. Xu and J. Read, *J. Power Sources*, 2011, **196**, 3906.
7 J. Read, M. Ervin, W. Behl, J. Wolfenstine, A. Driedger, D. Fostera and K. Mutolo, *J. Electrochem. Soc.*, 2003, **150**, A1351.

8 C. Xia, C. L. Bender, B. Bergner, K. Peppler and J. Janek, *Electrochem. Commun.*, 2013, **26**, 93.
9 J. G. Riess, *Colloids Surf., A*, 1994, **84**, 33.
10 J. G. Riess, *Chem. Rev.*, 2001, **101**, 2797.
11 M. P. Krafft and J. G. Riess, Chapter 11: Perfluorochemical-Based Oxygen Therapeutics, Contrast Agents, and Beyond, in *Fluorine Health*, ed. A. Tressaud and G. Haufe, Elsevier, 2008.
12 J. Lu, L. Li, J.-B. Park, Y.-K. Sun, F. Wu and K. Amine, *Chem. Rev.*, 2014, **114**, 5611.
13 C. O. Laoire, S. Mukerjee, E. J. Plichta, M. A. Hendrickson and K. M. Abraham, *J. Electrochem. Soc.*, 2011, **158**, A302.
14 H.-G. Jung, J. Hassoun, J.-B. Park, Y.-K. Sun and B. Scrosati, *Nat. Chem.*, 2012, **4**, 579.
15 R. Battlno, T. R. Rettich and T. Tominaga, *J. Phys. Chem. Ref. Data*, 1983, **12**, 163.
16 J. Read, K. Mutolo, M. Ervin, W. Behl, J. Wolfenstine, A. Driedger and D. Foster, *J. Electrochem. Soc.*, 2003, **150**, A1351.
17 R. Yazami, *US Pat.*, 0266907 A1, 2010.
18 M. Balaish, A. Kraytsberg and Y. Ein-Eli, *Phys. Chem. Chem. Phys.*, 2014, **16**, 2801.
19 B. D. McCloskey, D. S. Bethune, R. M. Shelby, G. Girishkumar and A. C. Luntz, *J. Phys. Chem. Lett.*, 2011, **2**, 1161.
20 V. S. Bryantsev, V. Giordani, W. Walker, M. Blanco, S. Zecevic, K. Sasaki, J. Uddin, D. Addison and G. V. Chase, *J. Phys. Chem. A*, 2011, **115**, 12399.
21 R. Black, S. Oh, J. Lee and T. Yim, *J. Am. Chem. Soc.*, 2012, **134**, 2902.
22 K. U. Schwenke, S. Meini, X. Wu, H. A. Gasteiger and M. Piana, *Phys. Chem. Chem. Phys.*, 2013, **15**, 11830.
23 K. R. Ryan, L. Trahey, B. J. Ingram and A. K. Burrell, *J. Phys. Chem. C*, 2012, **116**, 19724.
24 S. A. Freunberger, Y. Chen, N. E. Drewett, L. J. Hardwick, F. Bardé and P. G. Bruce, *Angew. Chem., Int. Ed.*, 2011, **50**, 8609.
25 V. Bryantsev and M. Blanco, *J. Phys. Chem. Lett.*, 2011, **2**, 379.
26 S. A. Freunberger, Y. Chen, Z. Peng, J. M. Griffin, L. J. Hardwick, F. Bardé, P. Novák and P. G. Bruce, *J. Am. Chem. Soc.*, 2011, **133**, 8040.
27 V. S. Bryantsev, J. Uddin, V. Giordani, W. Walker, D. Addison and G. V. Chase, *J. Electrochem. Soc.*, 2012, **160**, A160.
28 D. D. Lawson, J. Moacanin, K. V. Scherer, T. F. Terranova and J. D. Ingham, *J. Fluorine Chem.*, 1978, **12**, 221.
29 Y. Marcus, *Properties of Solvents*, Wiley, New York, 1998.
30 EL-CELL GmbH, http://www.el-cell.com/wp-content/uploads/manuals/ECC_AIR_manual.pdf, accessed online May 2015.
31 K. U. Schwenke, M. Metzger, T. Restle, M. Piana and H. A. Gasteiger, *J. Electrochem. Soc.*, 2015, **162**, A573.
32 P. Hartmann, D. Grübl, H. Sommer, J. Janek, W. G. Bessler and P. Adelhelm, *J. Phys. Chem. C*, 2014, **118**, 1461.
33 H. Ying and R. E. Baltus, *Ind. Eng. Chem. Res.*, 2007, **46**, 8166.
34 B. J. Bergner, A. Schu, K. Peppler, A. Garsuch and J. Janek, *J. Am. Chem. Soc.*, 2014, **136**, 15054.
35 S. A. Freunberger, Y. Chen, Z. Peng, J. M. Griffin, L. J. Hardwick, F. Bardé, P. Novák and P. G. Bruce, *J. Am. Chem. Soc.*, 2011, **133**, 8040.
36 J. Lu, L. Li, J.-B. Park, Y.-K. Sun, F. Wu and K. Amine, *Chem. Rev.*, 2014, **114**, 5611.
37 N. Madria, T. A. Arunkumar, N. G. Nair, A. Vadapalli, Y. W. Huang, S. C. Jones and V. P. Reddy, *J. Power Sources*, 2013, **234**, 277.
38 R. Younesi, S. Urbonaite, K. Edström and M. Hahlin, *J. Phys. Chem. C*, 2012, **116**, 20673.
39 R. Younesi, M. Hahlin and K. Edström, *ACS Appl. Mater. Interfaces*, 2013, **5**, 1333.
40 H. Bryngelsson, M. Stjerndahl, T. Gustafsson and K. Edström, *J. Power Sources*, 2007, **174**, 970.
41 Y. C. Lu, A. N. Mansour, N. Yabuuchi and Y. Shao-Horn, *Chem. Mater.*, 2009, **21**, 4408.
42 J. S. Oh, J. B. Park, E. Gil and G. Y. Yeom, *J. Phys. D: Appl. Phys.*, 2010, **43**, 425207.
43 H. Park, K. Kwon, J. Lee, K. Suh, O. Kwon, K. Cho, H. Park, K. Kwon, K. Cho, S. Park and O. Kwon, *Journal of Applied Physics*, 1994, **4596**, 4.
44 Y.-I. K. Hyung-Ho Park, K.-H. Kwon, S.-H. Lee, B.-H. Koak, S. Nahm, H.-T. Lee, K.-I. Cho and O.-J. Kwon, *ETRI J.*, 1994, **16**, 45.
45 G. M. Veith, J. Nanda, L. H. Delmau and N. J. Dudney, *J. Phys. Chem. Lett.*, 2012, **3**, 1242.
46 B. D. Mccloskey, A. Valery, A. C. Luntz, S. R. Gowda, G. M. Wallraff, J. M. Garcia, T. Mori and L. E. Krupp, *J. Phys. Chem. Lett.*, 2013, **4**, 2989.
47 E. Nasybulin, W. Xu, M. H. Engelhard, Z. Nie, S. D. Burton, L. Cosimbescu, M. E. Gross and J. Zhang, *J. Phys. Chem. C*, 2013, **117**, 2635.
48 D. Sharon, V. Etacheri, A. Garsuch, M. Afri, A. A. Frimer and D. Aurbach, *J. Phys. Chem. Lett.*, 2013, **4**, 127.
49 R. Younesi, G. M. Veith, P. Johansson, K. Edström and T. Vegge, *Energy Environ. Sci.*, 2015, 1905–1922.
50 R. A. Quinlan, Y.-C. Lu, Y. Shao-Horn and A. N. Mansour, *J. Electrochem. Soc.*, 2013, **160**, A669.